論 文

Probe로 급전되는 적층형 원형 마이크로스트립 2소자 배열안테나의 임피던스 및 상호결합 특성

正會員 李 勉 周* 正會員 南 相 郁*

Impedance and Mutual Coupling Characteristics of a Probe-Fed Stacked Circular Microstrip Two-Element Array Antenna

Myun Joo Park*, Sang Wook Nam* *Regular Members*

요 약

본 논문에서는 probe로 급전되는 적층형 마이크로스트립 2소자 배열 안테나의 임피던스 및 결합특성을 제시하였다. 안테나 구조의 해석에는 벡터 한켈 변환을 이용한 스펙트럴 영역법을 적용하였다. 또한 이 안테나의 임피던스 및 결합특성, 그리고 두 소자 안테나간의 거리에 따른 결합특성 변화등을 측정하여 그 결과를 제시한다. 끝으로, 해석을 통해 계산된 결과와 측정된 결과를 비교하여 두 결과가 잘 일치함을 보였다.

Abstract

In this paper, the coupling characteristics as well as the self and the mutual impedance of a two-element probe-fed stacked circular microstrip array antennas are presented. A full wave analysis for the structure is performed in the spectral domain using the vector Hankel transform(VHT). Also, we presented measured results for the impedance, the coupling characteristics of the antenna and the variation of the coupling with the distance between the two elements. Finally, the calculated and measured results are shown to agree well with each other through comparisons.

I. Introduction

Microstrip antennas have many advantages for practical applications ; flat profile, easy fabrication, easy integration with external circuits, etc. But their inherent narrow bandwidth is a major drawback in the applications which require a wide bandwidth. However, this shortcoming can be overcome by adding a parasitic element to the conventional microstrip antenna. The stacked microstrip antenna is an example of such approaches where a parasitic patch is located over/under the driven patch. Besides the wide bandwidth, this stacked structure has additional attractive features such as high gain, dual frequency operation, low sidelobe levels, and dual polarization[1].

*서울大學校 電子工學科
Dept. of Electronic Engineering, Seoul National Univ.
論文番號 : 93-178

Since a microstrip antenna is frequently used as an element of array structures, it is necessary to know the accurate coupling characteristics between them for the design of a good array antenna system. For the stacked microstrip array antenna, this knowledge of the coupling chracteristics is even more important, since such a coupling has much more influences on the performance due to their larger mutual coupling.

A full wave analysis of the probe-fed stacked circular microstrip antenna has been done successfully by Tulintseff[3], and the coupling characteristics between two probe-fed unstacked circular microstrip antennas were calculated by Habashy[4]. For the stacked rectangular microstrip antenna, the coupling characteristics between two elements have been analyzed by Terret[5]. However, to our knowledge, no analytical/experimental results have been reported for the coupling characteristics between stacked circular microstrip antennas although this type of antenna structure has been employed in several applications such as MSAT antenna for mobile telephone communication system[2].

In this paper, two element array of the probe fed stacked circular microstrip antennas is analyzed. The spectral domain method (SDM) via the vector Hankel transform(VHT) is used for the analysis. In addition to analysis, experiment is performed to verify the results of this analysis and close agreements are obtained between the theoretical and experimental results.

Ⅱ. Theory

1. Formulation of integral equations

Fig.1 shows the structure of a two-element array of the probe-fed stacked circular microstrip antennas together with the two independent cylindrical coordinate systems associated with each antenna A and B, which will be used in the analysis.

The first step in the analysis is to find the fields on each antenna. As for the antenna A, its field is the sum of the field by itself and the field

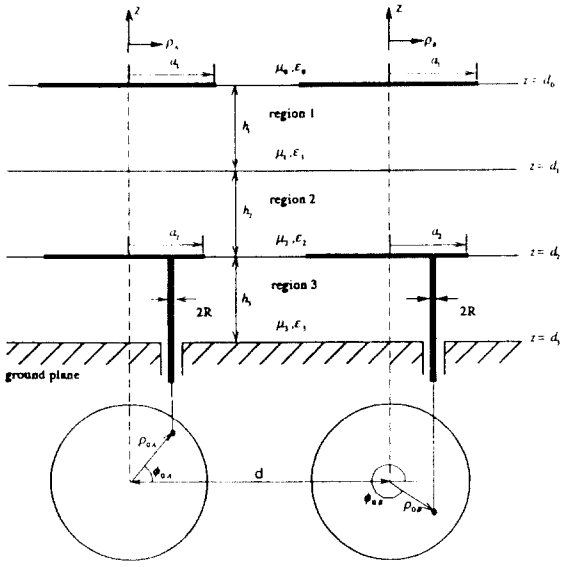

Fig 1. The structure of the two element array of the probefed stacked circular microstrip antenna and two circular cylindrical coordinate systems associated with antenna A and

by the antenna B. The self field is the field of a stacked microstrip antenna alone, which was calculated by Tulintseff[3]. In their analysis, the current on the surface of the feed probe was assumed to be uniform and to have the z-directed component only. The patches are assumed to be a perfect conductor having a negligible thickness and their suface currents are decomposed into $\hat{\rho}$ and $\hat{\phi}$ components. With these current distributions, the transverse electric field in the j-th region is given by eq.(1) from the results of Ref.[3].

$$\left[\bar{E}(\bar{\rho}_A,z)\right]_{T_j}=\sum_{m=-\infty}^{\infty}e^{im\phi_A}\int_0^{\infty}dk_\rho k_\rho\overline{\overline{H}}_m(k_\rho\rho)\left[\overline{\overline{G}}_{j1}(k_\rho,z,z'=d_0)\bar{\kappa}_{m1}^{A}(k_\rho)+\overline{\overline{G}}_{j2}(k_\rho,z,z'=d_2)\bar{\kappa}_{m2}^{A}(k_\rho)+\overline{\overline{G}}_{j3}(k_\rho,z)\bar{p}_m^{A}(k_\rho)\right] \tag{1}$$

The above integration is the inverse vector Hankel transform (VHT) whose kernel, $\overline{\overline{H}}_m(k_\rho\rho)$, can be found in Ref.[7]. The braketted quantity in the integrand is the spectral domain rep-

resentation of the m−th harmonic component of the transverse electric field $[\bar{E}(\bar{\rho}_1,z)]_{T_j}$. Also, the spectral domain dyadic Green's functions, $\overline{\overline{G}}_{ij}$'s can be found in Ref.[3]. $\bar{\kappa}_{m1}(k_\rho)$, $\bar{\kappa}_{m2}(k_\rho)$ represent the VHT's of the m−th harmonic component of the currents on the parasitic and driven patch, respectively, and $\bar{p}_m(k_\rho)$ is related to the probe current and given explicitly in [3].

Simiarly, the field on the antenna A due to the current on the antenna B can be calculated with the following conversion in the coordinate system. At first, the field by the antenna B is obtained in the coordinate system of B, which is the same as eq.(1) with all scripts A replaced by B. In applying the boundary conditions on the patches of the antenna A, it is convenient to represent all the field expressions in the coordinate system of A. Using the addition theorem for Bessel functions, given by eq.(2), the field on the antenna A by the antenna B is converted to the coordinate system of A as in eq.(3).

$$J_m(k_\rho\rho_B)e^{im\phi_B}=\sum_{n=-\infty}^{\infty}J_{n-m}(k_\rho d)J_n(k_\rho\rho_A)e^{in\phi_A} \tag{2}$$

$$\left[\bar{E}(\bar{\rho}_A,z)\right]_{Tj}=\sum_{m=-\infty}^{\infty}e^{im\phi_A}\int_0^{\infty}dk_\rho k_\rho\overline{\overline{H}}_m(k_\rho\rho)\left[\sum_{n=-\infty}^{\infty}J_{m-n}(k_\rho d)\left\{\overline{\overline{G}}_{j1}(k_\rho,z,d_0)\bar{\kappa}_{n1}^{B}(k_\rho)+\overline{\overline{G}}_{j2}(k_\rho,z,d_2)\bar{\kappa}_{n2}^{B}(k_\rho)\right\}+\overline{\overline{G}}_{j3}(k_\rho,z)\bar{p}_m'^{B}(k_\rho)\right] \tag{3}$$

The prime(′) in $\bar{p}_m'^{B}$ indicates that $\bar{p}_m^{B}$ is expressed in the coordinate system of A.

By combining the two field components given by eq.'s (1) and (3), the total tangential electric field on the antenna A is expressed as in eq.(4) for the m-th harmonic component.

$$\begin{aligned}\left[\bar{E}(\bar{\rho}_A,z)\right]_{Tjm}^{A}=&\int_0^{\infty}dk_\rho k_\rho\overline{\overline{H}}_m(k_\rho\rho_A)\left[\left\{\overline{\overline{G}}_{j1}(k_\rho,z,d_0)\bar{\kappa}_{m1}^{A}(k_\rho)\right.\right.\\&\left.\overline{\overline{G}}_{j2}(k_\rho,z,d_2)\bar{\kappa}_{m2}^{A}(k_\rho)+\overline{\overline{G}}_{j3}(k_\rho,z)\bar{p}_m^{A}(k_\rho)\right\}+\\&\sum_{n=-\infty}^{\infty}J_{m-n}(k_\rho d)\left\{\overline{\overline{G}}_{j1}(k_\rho,z,d_0)\bar{\kappa}_{n1}^{B}(k_\rho)+\right.\\&\left.\left.\overline{\overline{G}}_{j2}(k_\rho,z,d_2)\bar{\kappa}_{n2}^{B}(k_\rho)\right\}+\overline{\overline{G}}_{j3}(k_\rho,z)\bar{p}_m'^{B}(k_\rho)\right]\end{aligned} \tag{4}$$

Using the same procedure, the field on the antenna B can be obtained as in eq.(5).

$$\begin{aligned}\left[\bar{E}(\bar{\rho}_B,z)\right]_{Tjm}^{B}=&\int_0^{\infty}dk_\rho k_\rho\overline{\overline{H}}_m(k_\rho\rho_B)\left[\left\{\overline{\overline{G}}_{j1}(k_\rho,z,d_0)\bar{\kappa}_{m1}^{B}(k_\rho)\right.\right.\\&\left.\overline{\overline{G}}_{j2}(k_\rho,z,d_2)\bar{\kappa}_{m2}^{B}(k_\rho)+\overline{\overline{G}}_{j3}(k_\rho,z)\bar{p}_m^{B}(k_\rho)\right\}+\\&\sum_{n=-\infty}^{\infty}(-1)^{m-n}J_{m-n}(k_\rho d)\left\{\overline{\overline{G}}_{j1}(k_\rho,z,d_0)\bar{\kappa}_{n1}^{A}(k_\rho)+\right.\\&\left.\left.\overline{\overline{G}}_{j2}(k_\rho,z,d_2)\bar{\kappa}_{n2}^{A}(k_\rho)\right\}+\overline{\overline{G}}_{j3}(k_\rho,z)\bar{p}_m'^{A}(k_\rho)\right]\end{aligned} \tag{5}$$

The integral equation for the unknown currents on the patches can be obtained by imposing the conductor boundary condition on the patch, given by eq.(6).

$$\begin{aligned}&\left[\bar{E}(\bar{\rho}_A,z=z_j)\right]_{Tjm}^{A}=0,\quad \rho_A<a_j\\&\left[\bar{E}(\bar{\rho}_B,z=z_j)\right]_{Tjm}^{B}=0,\quad \rho_B<a_j\\&j=1,2.\quad z_1=d_0,z_2=d_2.\\&m=0,\pm1,\pm2,\cdots\end{aligned} \tag{6}$$

2. Moment method solution

The integral equations in eq.(6) are solved using the Galerkin's method. The basis functions used to expand the currents on the patches are the TM and TE mode currents on top of the cylindrical cavity with a magnetic sidewall. Also, the concept of an attachment mode current used in Ref.[3] is exploited to approximate the singular current near the probe-patch junction. Therefore, the current on each patch is expanded by the TE, TM mode currents and the attachment mode current as in eq.'s(7) and (8).

$$\bar{K}_m^{1}(\rho)=\sum_{p=1}^{P}A_{mp}^{1}\bar{\Psi}_{mp}^{1}(\rho)+\sum_{q=1}^{Q}B_{mq}^{1}\bar{\Phi}_{mq}^{1}(\rho) \tag{7}$$

$$\bar{K}_m^{2}(\rho)=\sum_{r=1}^{R}A_{mr}^{2}\bar{\Psi}_{mr}^{2}(\rho)+\sum_{s=1}^{S}B_{ms}^{2}\bar{\Phi}_{ms}^{2}(\rho)+\bar{K}_{m,att}^{2}(\rho) \tag{8}$$

where $\bar{\Psi}_{mp}(\rho)$, $\bar{\Phi}_{mq}(\rho)$ are the TM, TE mode currents, and $\bar{K}_{m,\,att}(\rho)$ is the attachment mode current.

Applying Galerkin's procedure to eq.(6) and using Parseval's theorem for the VHT[7], the final linear equations for the current expansion coefficients can be obtained by eq.'s (9) and (10).

$$\int_0^{\infty} dk_\rho k_\rho \overline{X}_{mf}^{Aj+}(k_\rho)\left[\overline{E}_T^j\left\{\overline{\psi}_m^A(k_\rho),\overline{\phi}_m^A(k_\rho)\right\}+\sum_{n=-M}^{M} J_{m-n}(k_\rho d)\overline{E}_T^j\left\{\overline{\psi}_m^B(k_\rho),\overline{\phi}_m^B(k_\rho)\right\}\right]$$
$$=-\int_0^{\infty} dk_\rho k_\rho \overline{X}_{mf}^{Aj+}(k_\rho)\left[\overline{E}_T^j\left\{\overline{K}_{m,at}^A\right\}+\sum_{n=-M}^{M} J_{m-n}(k_\rho d)\overline{E}_T^j\left\{\overline{K}_{m,at}^B\right\}\right]$$
$$-\int_0^{\infty} dk_\rho k_\rho \overline{X}_{mf}^{Aj+}(k_\rho)\left[\overline{E}_T^j\left\{\overline{p}_m^A\right\}+\overline{E}_T^j\left\{\overline{p}_m'^B\right\}\right] \quad (9)$$

$$\int_0^{\infty} dk_\rho k_\rho \overline{X}_{mf}^{Bj+}(k_\rho)\left[\overline{E}_T^j\left\{\overline{\psi}_m^B(k_\rho),\overline{\phi}_m^B(k_\rho)\right\}+\sum_{n=-M}^{M}(-1)^{m-n} J_{m-n}(k_\rho d)\overline{E}_T^j\left\{\overline{\psi}_m^A(k_\rho),\overline{\phi}_m^A(k_\rho)\right\}\right]$$
$$=-\int_0^{\infty} dk_\rho k_\rho \overline{X}_{mf}^{Bj+}(k_\rho)\left[\overline{E}_T^j\left\{\overline{K}_{m,at}^B\right\}+\sum_{n=-M}^{M}(-1)^{m-n} J_{m-n}(k_\rho d)\overline{E}_T^j\left\{\overline{K}_{m,at}^A\right\}\right]$$
$$-\int_0^{\infty} dk_\rho k_\rho \overline{X}_{mf}^{Aj+}(k_\rho)\left[\overline{E}_T^j\left\{\overline{p}_m^B\right\}+\overline{E}_T^j\left\{\overline{p}_m'^A\right\}\right] \quad (10)$$

where $j=1,2$, $m=0, \pm1, \pm2, \ldots \pm M$, and superscript + means a complex conjugate transpose.

In the above equations, the testing function $\overline{X}(k_\rho)$ is the same as the basis function in the Galerkin's method, which is given by eq.(11).

$$\overline{X}(k_\rho) = \overline{\psi}(k_\rho) \text{ or } \overline{\phi}(k_\rho) \quad (11)$$

Also, $E_T^j\{*\}$'s in eq.'s (9) and (10) are the tangential electric fields on the patch j due to the expansion function current, attachment mode current, and current on the feed probe. Their explicit expressions are given by eq.(12).

$$\overline{E}_T^j\left\{\overline{\psi}_m^\chi(k_\rho),\overline{\phi}_m^\chi(k_\rho)\right\}=\overline{\overline{G}}_{j1}(k_\rho, z=z_j, d_0)\left[\sum_{p=1}^{P} A_{mp}^{\chi 1}\overline{\psi}_{mp}^{\chi 1}(k_\rho)+\sum_{q=1}^{Q} B_{mq}^{\chi 1}\overline{\psi}_{mq}^{\chi 1}(k_\rho)\right]+$$
$$\overline{\overline{G}}_{j2}(k_\rho, z=z_j, d_2)\left[\sum_{r=1}^{R} A_{mr}^{\chi 2}\overline{\psi}_{mr}^{\chi 2}(k_\rho)+\sum_{s=1}^{S} B_{ms}^{\chi 2}\overline{\psi}_{ms}^{\chi 2}(k_\rho)\right]$$
$$\overline{E}_T^j\left\{\overline{K}_{m,at}^\chi\right\}=\overline{\overline{G}}_{j2}(k_\rho, z=z_j, d_2)\overline{K}_{m,at}^\chi(k_\rho) \quad (12)$$

$$\overline{E}_T^j\left\{\overline{p}_m^\chi\right\}=\overline{\overline{G}}_{j3}(k_\rho, z=z_j)\overline{p}_m^\chi(k_\rho)$$

χ = A, B

The current distribution on the patches can be obtained from the solution of these $2*(2*M+1)*(P+Q+R+S)$ linear equations.

3. Calculation of impedance

To obtain the self impedance and the mutual impedance of the antenna, the following variational formulas are used.

$$Z_{AA}=-\frac{1}{I_A^2}\int_{Probe\ A}\overline{E}_A\bullet\overline{J}_A dS_A \quad (13)$$

$$Z_{AB}=-\frac{1}{I_A I_B}\int_{Probe\ B}\overline{E}_A\bullet\overline{J}_B dS_B \quad (14)$$

In the above equations, $\overline{E}_A$ means the electric field due to the uniform current along the feed probe of the antenna A with the antenna B open circuited. Also, $\overline{J}_A$, $\overline{J}_B$ means the surface current density on the surface of the antenna A and B whose terminal currents are denoted by I_A and I_B.

Calculating the electric fields and performing the integtration as indicated in eq.'s (13) and (14), the impedance parameters of the antenna are calculated by eq.'s (15), (16).

$$Z_{AA}=-\frac{2\pi}{I_A^2}\sum_{m=-\infty}^{\infty}\int_0^{\infty} dk_\rho k_\rho\left[p_m^{A*}(k_\rho)\left\{\eta_{3,1}^{TM}(k_\rho)\left[\overline{K}_{m1}^A(k_\rho)\right]_\rho+\eta_{3,2}^{TM}(k_\rho)\left[\overline{K}_{m2}^A(k_\rho)\right]_\rho\right\}+p_m'^{A*}(k_\rho)\left\{\eta_{3,1}^{TM}(k_\rho)\left[\overline{K}_{m1}^B(k_\rho)\right]_\rho+\eta_{3,2}^{TM}(k_\rho)\left[\overline{K}_{m2}^B(k_\rho)\right]_\rho\right\}\right]+\frac{\eta_3}{4}k_3 h_3 J_0(k_3 R)H_0^{(1)}(k_3 R)+$$
$$\frac{1}{I_A}\sum_{m=-\infty}^{\infty} e^{-jm\phi_{0A}}\frac{J_0(k_3 R)J_m(k_3\rho_{0A})}{J_m'(k_3 a_2)}\times$$
$$\int_0^{\infty} dk_\rho k_\rho p_m^{A*}(k_\rho)J_m'(k_\rho a_2)\frac{k_3}{k_{3z}^2}\eta_{3,2}^{TM}(k_\rho) \quad (15)$$

$$Z_{AB} = -\frac{2\pi}{I_A I_B}\sum_{m=-\infty}^{\infty}\int_0^{\infty} dk_\rho k_\rho \Big[p_m^{B*}(k_\rho)\Big\{\eta_{3,1}^{TM}(k_\rho)\Big[\overline{K}_{m1}^{B}(k_\rho)\Big]_\rho + \eta_{3,2}^{TM}(k_\rho)\Big[\overline{K}_{m2}^{B}(k_\rho)\Big]_\rho\Big\} + p_m'^{B*}(k_\rho)\Big\{\eta_{3,1}^{TM}(k_\rho)\Big[\overline{K}_{m1}^{A}(k_\rho)\Big]_\rho + \eta_{3,2}^{TM}(k_\rho)\Big[\overline{K}_{n2}^{A}(k_\rho)\Big]_\rho\Big\}\Big] + \frac{\eta_3}{4}k_3 h_3 J_0(k_3 t) J_0(k_3 R) H_0^{(1)}(k_3 R) + \frac{1}{I_B}\sum_{m=-\infty}^{\infty} e^{-im\phi_{0A}} \frac{J_0(k_3 R) J_m(k_3 \rho_{0A})}{J_m'(k_3 a_2)} \times \int_0^{\infty} dk_\rho k_\rho p_m'^{B*}(k_\rho) J_m'(k_\rho a_2) \frac{k_3}{k_{3z}^2} \eta_{3,2}^{TM}(k_\rho) \tag{16}$$

The explicit expressions for $\eta_{i,j}^{TM}$'s can be found in Ref.[3].

Ⅲ. Results and discussions

Based on the theory presented in the previous section, several characteristics of a two-element array of stacked circular microstrip antennas can be obtained. For the numerical evaluation of improper integrals appearing in eq.'s (10), (15), and (16), the integral paths are deformed just below the real axis to avoid singularities on the real axis. In the deformed path, the imaginary part of k_ρ is fixed at $10^{-3}\,k_0$.

In calculating impedance parameters we have omitted the second term involving $H_0^{(1)}(k_3R)$ in eq.'s (15) and (16). The omitted term appears as a part of the probe self impedance and represents the impedance of the parallel plate waveguide fed by probe[3]. Even though the term shows the resistance component as well as the reactance component, it is well known that the probe self impedance has a reactive component only. This inconsistency is thought to have occurred due to the incompleteness of our feed model. We assumed uniform current on the feed probe with magnitude equal to the terminal current, so that open-circuiting a terminal means no current on the corresponding probe. However, some currents on the probe and the corresponding attachment current on the driven patch must exist in real situations. We feel that a more elaborated feeder model such as the magnetic frill model is needed to correct this problem.

In Calculation, we used M = 1, P = Q = R = S = 4 for the basis functions. The structure parameter of the antenna element used for the simulation and the measurement is given as follows ; $a_2 = 1.3cm$, $a_1 = 1.01a_2$, $h_1 = h_3 = 0.16cm$, $h_2 = 0.5cm$, $\varepsilon_{r3} = \varepsilon_{r1} = 2.58$, $\varepsilon_{r2} = 1.0$, and $\rho_{0A} = \rho_{0B} = 0.8a_2$.

Fig.2 shows the Smith chart plot for the S11of the coupled antenna together with the measured data, when the spacing between two antenna element is $d = 2.07a_2$. Compared with the measured data, the calulated results are accurate near resonance, but deviates a little away from the resonance. This is considered to be due to the choice of the basis functions. Since the basis functions are the resonance mode currents of the cylindrical cavity, they seem to be less adequate to represent the patch current in the off-resonance condition.

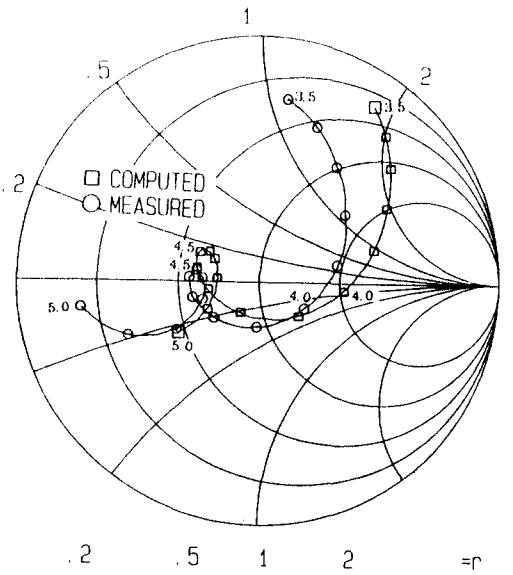

Fig 2. The smith chart representing the S11 characteristic of the antenna in Fig.1.
($a_2 = 1.3cm$, $a_1 = 1.01a_2$, $h_1 = h_3 = 0.16cm$, $h_2 = 0.5cm$, $\varepsilon_{r3} = \varepsilon_{r1} = 2.58$, $\varepsilon_{r2} = 1.0$, $\rho_{0A} = \rho_{0B} = 0.8a_2$, $\phi_{0A} = \phi_{0B} = \pi/2$, $d = 2.07a_2$)

In Fig.3, the return loss and the mutual coupling are presented as a function of the frequency. The calculated results show good agreements with the measured data.

In Fig.4, the mutual coupling between the two element antennas is plotted for two different feeder positions as a function of the spacing between the two element antenna. Also, the measured coupling data for the unstacked circular patch antennas are presented for the comparison. When the two element antennas are very close to each other ($d < \sim 3.5a_2$), the E-plane coupling is larger than the H-plane coupling. As the distance between the antennas is increased, the E plane

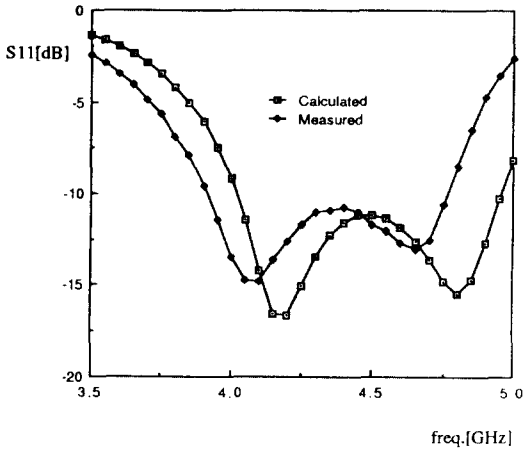

(a)

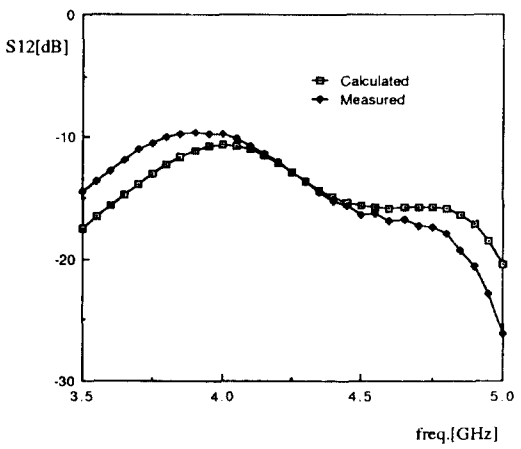

(b)

Fig 3. (a) Return loss and (b) Coupling versus frequency of the antenna in Fig.1.
($a_2 = 1.3cm$, $a_1 = 1.01a_2$, $h_1 = h_3 = 0.16cm$, $h_2 = 0.5cm$, $\varepsilon_{r3} = \varepsilon_{r1} = 2.58$, $\varepsilon_{r2} = 1.0$, $\rho_{0A} = \rho_{0B} = 0.8a_2$, $\phi_{0A} = \phi_{0B} = \pi/2$, $d = 2.07a_2$)

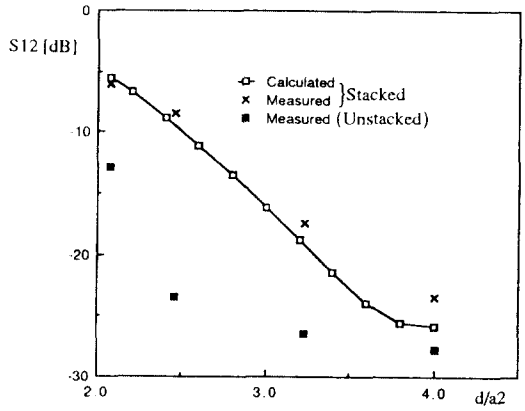

(a)

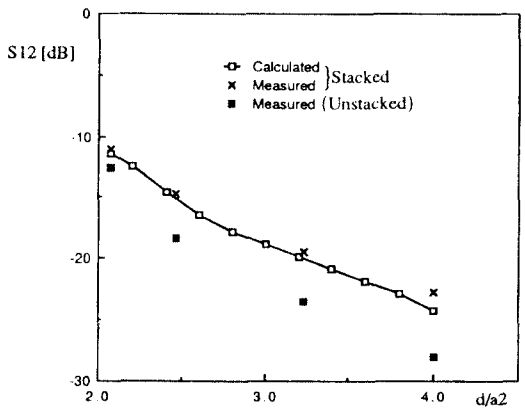

(b)

Fig 4. (a) E plane ($\phi_{0A} = \phi_{0B} = 0$) and (b) H plane ($\phi_{0A} = \phi_{0B} = \pi/2$) Coupling versus element spacing.
($a_2 = 1.3cm$, $a_1 = 1.01a_2$, $h_1 = h_3 = 0.16cm$, $h_2 = 0.5cm$, $\varepsilon_{r3} = \varepsilon_{r1} = 2.58$, $\varepsilon_{r2} = 1.0$, $\rho_{0A} = \rho_{0B} = 0.8a_2$)

coupling decreases more rapidly. As a result, at large distances($d > \sim 3.5a_2$), the coupling in the H-plane is slighly larger than the E-plane coupling. The same results can be observed in the case of the stacked rectangular microstrip antennas in Ref.[5]. Therefore, to reduce the effect of the mutual coupling in the stacked microstrip antenna arrays in which the element antennas are very close to one another, the H-plane feeding is recommended. However, when the distance between elements is far enough, the E-plane feeding is slightly better.

References

1. J. R. James and P. S. Hall Ed., *Handbook of Microstrip Antennas*, Chap.6, London, U.K.: Peter Peregrinus, 1981.
2. F. Schmidt, "MSAT Mobile Eletronically Steered Phased Array Antenna developement," Ball Aerospace Group, USA.
3. A. N. Tulintseff, S. M. Ali and J. A. Kong, "Input Impedance of a Probe-Fed Stacked Circular Microstrip Antenna," *IEEE Trans. Antennas Propagat.*, vol. AP-39, pp. 381-390, Mar. 1991.
4. T. M. Habashy, S. M. Ali and J. A. Kong, "Impedance and Radiation Pattern of Two Coupled Circular Microstrip Disk Antennas," *J. Appl. Phys.*, vol. 54, no.2, pp. 493-506, Feb.1983.
5. C. Terret, S. Assailly, K. Mahdjoubi, and M. Edimo, "Mutual Coupling Between Stacked Square Microstrip Antennas Fed on Their Diagonal," *IEEE Trans. Antennas Propagat.*, vol. AP-39, pp. 1049-1051, July 1991.
6. S. M. Ali, T. M. Habashy and J. A. Kong, "Resonance in Two Coupled Circular Microstrip Disk Resonators," *J. Appl. Phys.*, vol. 53, no.9, pp. 6418-6428, Sep. 1983.
7. W. C. Chew and T. M. Habashy, "The Use of Vector Transforms in Solving Some Electromagnetic Problems," *IEEE Trans. Antennas Propagat.*, vol. AP-34, pp. 871-879, July 1986.

朴 勉 周(Myun Joo Park) 正會員
1968年 2月 10日生
1991年 2月 : 서울大學校 電子工學科 卒業(工學士)
1993年 2月 : 서울大學校 大學院 電子工學科 卒業(工學碩士)
1993年~現在 : 서울大學校 大學院 電子工學科 博士課程 在學中
※主關心分野 : 안테나 및 受動回路의 數値解析

南 相 郁(Sangwook Nam) 正會員
1959年 2月 2日生
1981年 2月 : 서울大學校 電子工學科 卒業(工學士)
1983年 2月 : 韓國科學技術院 電氣·電子工學科 卒業(工學碩士)
1983年 2月 ~ 1986年 8月 : 金星社 中央研究所(主任研究員)
1989年 5月 : 美國 Texas 洲立大學校 電氣工學科 卒業(工學博士)
1989年 6月 ~ 1989年 9月 : 美國 Texas 洲立大學校 Post-Doc.(研究員)
1989年 9月 ~ 1990年 1月 : 金星精密 研究所(先任研究員)
1990년 2월 ~ 現在 : 서울大學校 工科大學 電子工學科 助教授
※主關心分野 : 電磁波 解析, 마이크로波 測定 및 回路設計